ISSN (e): 2250 – 3005 || Vol, 04 || Issue, 7 || July – 2014 ||
International Journal of Computational Engineering Research (IJCER)

Radiation and Soret Effects to MHD Flow in Vertical Surface with Chemical reaction and Heat generation through a Porous Medium

[1]Srinathuni Lavanya, [2]D Chenna Kesavaiah
[1]*Department of H&S, Narayana Engineering & Technical Campus, Jafarguda, Hayatnagar, R.R.Dist, T.S, India.*
[2]*Department of H & BS, Visvesvaraya College of Engg & Tech, MP Patelguda, Ibrahimpatnam, R.R.Dist, T.S, India*

ABSTRACT
The present paper is the effects of radiation, chemical reactions and thermo Diffusion (Soret effect) to MHD flow of an electrically conducting, incompressible, viscous fluid past an impulsively moving isothermal vertical plate through porous medium in the presence of uniform suction. Thermo diffusion is one of the mechanisms in transport phenomena in which molecules are transported in a multi component mixture driven by temperature gradients. A flow of this type represents a new class of boundary layer flow at a surface of finite length. The equations governing the flow field are solved by analytical method. The velocity, temperature, concentration and skin friction have been evaluated for variation in the different governing parameters.

KEYWORDS: *Chemical reaction, Heat generation/absorption, Radiation, Soret number, MHD, Porous medium, Radiation*

I. INTRODUCTION

Thermo diffusion along with molecular diffusion occurs in many engineering systems and in nature. Thermo diffusion has a great effect on the concentration distribution in a multi component mixture. The variations of composition and temperature may either lessen or enhance the separation in mixtures. The thermo diffusion phenomenon also plays a major role in the hydrodynamic instability analysis in mixtures, investigations of mineral migration, the mass transport modeling in living matters, and composition variation studies in hydrocarbon reservoirs. Diffusion is one of the major mechanisms of transport phenomena. Molecular diffusion is the movement of molecules from a higher to lower chemical potential. Thermo diffusion and pressure diffusion are additional ways in which molecules are transported in a multi component mixture driven by temperature and pressure gradients, respectively. The thermo diffusion phenomenon was discovered by Ludwig [1] and Soret [2], and named as the Soret effect. The Soret coefficient is the ratio of the thermo diffusion coefficient to the molecular diffusion coefficient.

Furthermore, the study of thermo hyaline instability with thermo diffusion in a fluid saturated porous medium is of importance in geophysics, ground water hydrology, soil science, oil extraction. The reason is that the earth's crust is a porous medium saturated by a mixture of different types of fluids such as oil, water, gases and molten form of ores dissolved in fluids. Thermal gradients present between the interior and exterior of the earth's crust may help convection to set in. The thermal gradient in crude oil can have a strange effect on the distribution of petroleum components in an oil deposit. The thermal gradient causes the Soret effect which makes the larger molecule components to have a tendency to rise, while smaller molecule components go down to the bottom of the well. However, gravity causes the heavy components in a fluid to fall and the lighter ones to rise. This means that the distribution of components in a given well is neither consistent nor readily predictable. Pal and Talukdar [3] analyzed the combined effect of mixed convection with thermal radiation and chemical reaction on MHD flow of viscous and electrically conducting fluid past a vertical permeable surface embedded in a porous medium is analyzed. Mukhopadhyay [4] performed an analysis to investigate the effects of thermal radiation on unsteady mixed convection flow and heat transfer over a porous stretching surface in porous medium. Hayat et al. [5] analyzed a mathematical model in order to study the heat and mass transfer characteristics in mixed convection boundary layer flow about a linearly stretching vertical surface in a porous

medium filled with a viscoelastic fluid, by taking into account the diffusion thermo (Dufour) and thermal-diffusion (Soret) effects. Bhavana et.al [6]. The Soret effect on free convective unsteady MHD flow over a vertical plate with heat source. Chenna Kesavaiah et.al [7] Radiation and Thermo - Diffusion effects on mixed convective heat and mass transfer Flow of a viscous dissipated fluid over a vertical surface in the presence of chemical reaction with heat source.

MHD flows has received the attention of several researchers due to its diverse applications in many branches of sciences and technology such as in planetary fluid dynamics, power generation systems, nuclear reactor thermal dynamics and electromagnetic materials processing. On the other hand, MHD flows with combined heat and mass transfer has numerous applications in chemical, mechanical and biological sciences. Some important application are stellar and solar structures cooling of nuclear reactors, interstellar matter, liquid metals fluid, power generation system, radio propagation and aerodynamics.

The study of heat generation or absorption in moving fluid is important in problems dealing with dissociating fluids. Possible heat generation effect may alter the temperature distribution; consequently, the particle deposition rate in nuclear reactors, electronic chips and semi conductor wafers. Rahman et al. [8] studied thermo-micropolar fluid flow along a vertical permeable plate with uniform surface heat flux in the presence of heat generation. Ibrahim et al. [9] found the analytic solution of MHD mixed convection heat and mass transfer over an isothermal, inclined permeable stretching plate immersed in a uniform porous medium in the presence of chemical reaction, internal heating, Dufour effect and Hall effects. Pal and Chatterjee [10] studied heat and mass transfer in MHD non-Darcian flow of a micropolar fluid over a stretching sheet embedded in a porous media with non-uniform heat source and thermal radiation. Cortell [11] investigated theoretically the effect of viscous dissipation as well as radiation on the thermal boundary layer flows over non-linearly stretching sheets considering prescribed surface temperature and heat flux. Raptis and Perdikis [12] studied numerically the steady two dimensional flow of an incompressible viscous and electrically conducting fluid over a non-linear semi-infinite stretching in the Presence of a chemical reaction and under the influence of magnetic field. Rajagopal *et al.* [13] studied a Falkner-Skan flow field of a second-grade viscoelastic fluid. Shit and Haldar [14] investigated the effects of thermal radiation and Hall current on MHD free-convective flow and mass transfer over a stretching sheet with variable viscosity in the Presence of heat generation/absorption.

Therefore the objective of the present paper is to study the MHD heat transfer flow of a Newtonian fluid moving vertical surface with heat generation or absorption by considering the radiation effect along with Soret effect, uniform heat and mass flux and chemical reaction.

II. FORMULATION OF THE PROBLEM

We consider the steady, two-dimensional laminar, incompressible flow of a chemically reacting, viscous fluid on a continuously moving vertical surface in the presence of a uniform magnetic field, radiation absorption with heat generation, uniform heat and mass flux effects issuing a slot and moving with uniform velocity in a fluid at rest. Let the x-axis be taken along the direction of motion of the surface in the upward direction and y-axis is normal to the surface. The temperature and concentration levels near the surface are raised uniformly. The induced magnetic field, viscous dissipation is assumed to be neglected. Now, under the usual Boussinesq's approximation, the flow field is governed by the following equations.

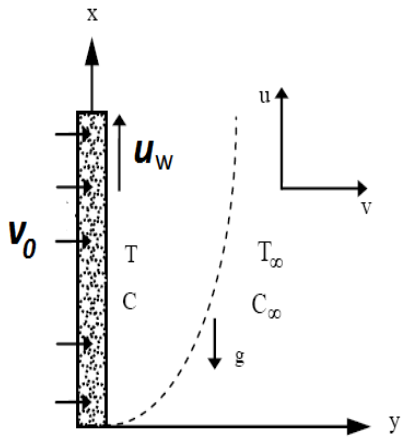

Flow configuration and coordinate system

Continuity equation

$$\frac{\partial u}{\partial x}+\frac{\partial v}{\partial y}=0 \tag{1}$$

Momentum equation

$$u\frac{\partial u}{\partial x}+v\frac{\partial u}{\partial y}=g\beta\left(T'-T_{\infty}'\right)+g\beta^{*}\left(C'-C_{\infty}'\right)+\nu\frac{\partial^{2}u}{\partial y^{2}}-\frac{\sigma B_{0}^{2}}{\rho}u-\frac{\nu}{K_{p}}u \tag{2}$$

Energy equation

$$\rho C_{p}\left(u\frac{\partial T'}{\partial x}+v\frac{\partial T'}{\partial y}\right)=k\frac{\partial^{2}T'}{\partial y^{2}}-\frac{\partial q_{r}}{\partial y}-Q_{0}\left(T'-T_{\infty}'\right) \tag{3}$$

$$u\frac{\partial C'}{\partial x}+v\frac{\partial C'}{\partial y}=D_{M}\frac{\partial^{2}C'}{\partial y^{2}}-Kr'\left(C'-C_{\infty}'\right)+D_{T}\frac{\partial^{2}T'}{\partial y^{2}} \tag{4}$$

The relevant boundary conditions are

$$\begin{aligned}&u=u_{w},v=-v_{0}=const<0\\&\frac{\partial T}{\partial y}=-\frac{q}{k},\ \frac{\partial C}{\partial y}=-\frac{j''}{D}\qquad at\quad y=0\\&u\to 0,T\to T_{\infty},C\to C_{\infty}\qquad as\quad y\to\infty\end{aligned} \tag{5}$$

The radiative heat flux q_r is given by equation (5) in the spirit of Cogly et.al [15]

$$\frac{\partial q_{r}}{\partial y}=4(T'-T_{\infty}')I\qquad\text{where } I=\int_{0}^{\infty}K_{\lambda w}\frac{\partial e_{b\lambda}}{\partial T^{*}}d\lambda,$$

$K_{\lambda w}$ – is the absorption coefficient at the wall and $e_{b\lambda}$ – is Planck's function, I is absorption coefficient

In order to write the governing equations and the boundary conditions the following non dimensional quantities are introduced.

$$u=\frac{u}{u_{w}},Y=\frac{yv_{0}}{\nu},\ T=\frac{T'-T_{\infty}'}{\left(\frac{q\nu}{kv_{0}}\right)},C=\frac{C'-C_{\infty}'}{\left(\frac{j''\nu}{kv_{0}}\right)},k=\frac{K_{p}v_{0}^{2}}{\nu^{2}},M=\frac{\sigma B_{0}^{2}\nu}{\rho v_{0}^{2}},Q=\frac{\nu Q_{0}}{\rho C_{p}v_{0}^{2}}$$

$$\Pr=\frac{\mu C_{p}}{k},Kr=\frac{Kr'\nu}{v_{0}^{2}},Q_{l}=\frac{Q_{l}'j''\nu}{qv_{0}^{2}\rho C_{p}},Gr=\frac{\nu g\beta\left(\frac{q\nu}{kv_{0}}\right)}{u_{w}v_{0}^{2}},Sc=\frac{\nu}{D_{M}},Gc=\frac{\nu g\beta^{*}\left(\frac{j''\nu}{kv_{0}}\right)}{u_{w}v_{0}^{2}} \tag{6}$$

$$Du=\frac{D_{M}K_{T}j''}{c_{s}c_{p}\nu q\rho C_{p}},R=\frac{4q\nu I}{kv_{0}},S_{0}=\frac{qD_{T}}{\nu j''}$$

Where u,v are the velocity along the x,y -axis, is constant obtained after integration conservation of mass in pre-non dimensional form not mentioned, ν is the kinematic viscosity, g is the acceleration due to gravity, T' is the temperature of the fluid, is the coefficient of volume expansion, C_p is the specific heat at constant pressure, is a constant, σ is the Stefan-Boltzmann constant, T_w' exceeds the free steam temperature T_{∞}', C' is

the species concentration, is the wall temperature, C'_w is the concentration at the plate, T'_∞ is the free steam temperature far away from the plate, C'_∞ is the free steam concentration in fluid far away from the plate, $\Pr$ is the Prandtl number, Gr is the Grashoff number, k is the thermal conductivity of the fluid, B_0 is uniform magnetic field strength, M is the magnetic field parameter which is the ratio of magnetic force to the inertial force. It is a measure of the effect of flow on the magnetic field. The term $Q_0 (T' - T'_\infty)$ is assumed to be the amount of heat generated or absorbed per unit volume. Q_0 is a constant, which may take on either positive or negative values.

III. SOLUTION OF THE PROBLEM

In view of (6) the equations (2), (3) and (4) are reduced to the following non-dimensional form

$$\frac{d^2U}{dY^2} + \frac{dU}{dY} - \left(M + \frac{1}{K}\right)U = -GrT - GcC \tag{7}$$

$$\frac{d^2T}{dY^2} + \Pr\frac{dT}{dY} - (Q + R)\Pr T = 0 \tag{8}$$

$$\frac{d^2C}{dY^2} + Sc\frac{dC}{dY} - KrScC + ScS_o\frac{d^2T}{dY^2} = 0 \tag{9}$$

The corresponding boundary conditions can be written as

$$\begin{aligned} &U = 1, \quad \frac{\partial T}{\partial Y} = -1, \quad \frac{\partial C}{\partial Y} = -1 \qquad at\ Y = 0 \\ &U \to 0, T \to 0, C \to 0 \qquad as\ Y \to \infty \end{aligned} \tag{10}$$

Where Gr is the thermal Grashof number, Gc is the solutal Grashof number, $\Pr$ is the fluid Prandtl number, Sc is the Schmidt number Kr is the chemical reaction, Q is Heat source parameter, M is the Magnetic parameter, S_0 is the Soret number and R is the Radiation Parameter.

The study of ordinary differential equations (7), (8) and (9) along with their initial and boundary conditions (10) have been solved by using the method of ordinary linear differential equations with constant coefficients. We get the following analytical solutions for the velocity, temperature and concentration.

$$U = J_1 e^{m_2 y} + J_2 e^{m_2 y} + J_3 e^{m_4 y} + J_4 e^{m_6 y}$$

$$T = B_1 e^{m_2 y}$$

$$C = Z_1 e^{m_2 y} + Z_2 e^{m_4 y}$$

The computed solution for the velocity is valid at some distance from the slot, even though suction is applied from the slot onward. This is due to the assumption that velocity field is independent of the distance parallel to the plate. The fluids considered in this study are air (Pr = 0.71) and water (Pr = 7.0).

Skin friction

$$\tau = \left(\frac{\partial U}{\partial y}\right)_{y=0}$$

$$= J_1 m_2 + J_2 m_2 + J_3 m_4 + J_4 m_6$$

Nusselt number

$$Nu = \left(\frac{\partial T}{\partial y}\right)_{y=0} = B_1 m_2$$

Sherwood number

$$Sh = \left(\frac{\partial C}{\partial y} \right)_{y=0} = Z_1 m_2 + Z_2 m_4$$

APPENDIX

$$m_2 = -\left(\frac{Sc + \sqrt{Sc^2 + 4KrSc}}{2} \right) \quad m_4 = -\left(\frac{\Pr + \sqrt{\Pr^2 + 4(Q+R)\Pr}}{2} \right) \quad m_2 = -\left(\frac{1 + \sqrt{1 + 4\left(M + \frac{1}{K}\right)}}{2} \right)$$

$$\alpha = (Q+R)\Pr \quad B_1 = -\frac{1}{m_2}, Z_1 = -\frac{B_1 m_2^2 Sc S_o}{m_2^2 + Scm_2 - KrSc} \quad Z_2 = -\left(\frac{1 + Z_1 m_1}{m_4} \right)$$

$$J_1 = -\frac{GrB_1}{m_2^2 + m_2 - \left(M + \frac{1}{K}\right)} \quad J_2 = -\frac{GcZ_1}{m_2^2 + m_2 - \left(M + \frac{1}{K}\right)} \quad J_3 = -\frac{GcZ_2}{m_4^2 + m_4 - \left(M + \frac{1}{K}\right)}$$

$$J_4 = (1 - J_1 - J_2 - J_3)$$

IV. RESULTS AND DISCUSSION

The variation of non-dimensional velocity U for different values of Grashof number (Gr), Solutal Grashof number (Gc), Porosity permeability (K), Chemical reaction parameter (Kr), Magnetic parameter (M), Prandtl number $(\Pr)$, Heat source parameter (Q), Radiation parameter (R) Soret number (S_0) and Schmidt number (Sc) are shown in figures (1) - (10).

Figure (1) shows the influence of thermal buoyancy force parameter (Gr) on the velocity. As can be seen from this figure, the velocity profile increases with increases in the values of the thermal buoyancy. We actually observe that the velocity overshoot in the boundary layer region. Buoyancy force acts like a favourable pressure gradient which accelerates the fluid within the boundary layer therefore the solutal buoyancy force parameter (Gc) has the same effect on the velocity shown in figure (2) as Gr. Figure (3) shows that the axial velocity increases with a rise in permeability parameter (K). Moreover, for small permeability, the axial velocity reduces faster than when the permeability is higher. Figure (4) depict effect of chemical reaction on the flow variables is shown. In figure (4) velocity is clearly boosted with stronger chemical reaction i.e. as the chemical reaction parameter (Kr) increases profiles are lifted continuously throughout the boundary layer, transverse to the plate. A distinct velocity escalation occurs near the wall after which profiles decay smoothly to the stationary value in the free stream. Chemical reaction therefore boosts momentum transfer i.e. accelerates the flow. Figure (5) reveals that axial velocity decreases as Magnetic parameter (M) increases. This may be attributed to the fact that an increase in M signifies an enhancement of Lorentz force, thereby reducing the magnitude of the velocity. This figure further indicates that blood velocity in the capillary decreases with increase in distance from the lower wall of the capillary. Figure (6) illustrates the effect of Prandtl number $(\Pr)$ on the velocity. It is noticed that as the Prandtl number $(\Pr)$ increases, the velocity decreases. As seen in the earlier cases, far away from the plate, the effect is much significant. Figure (7) illustrate the variation of velocity with the effects of heat absorption parameter (Q). The velocity values are clearly reduced with increasing Q; again an overshoot is computed close to the plate both in the presence and absence of heat source. Heat source

however suppresses the overshoot. Figure (8) show the effect of radiation parameter (R) on the velocity it is observed that the velocity decrease as the radiation parameter (R) increases. This result qualitatively agrees with expectations. Figure (9) shows the variation of the velocity boundary-layer with the Soret number (Sr). It is found that the velocity boundary layer thickness increases with an increase in the Soret number. Figure (10) illustrates the effect of the Schmidt number (*Sc*) on the velocity. The Schmidt number (Sc) embodies the ratio of the momentum diffusivity to the mass (species) diffusivity. It physically relates the relative thickness of the hydrodynamic boundary layer and mass-transfer (concentration) boundary layer. It is noticed that as Schmidt number (Sc) increases the velocity field decreases.

Figures (11) – (13) give some characteristic temperature profiles for different values of Prandtl number (Pr), heat source parameter (Q) and radiation parameter (R). Figure (11) presents the change in the temperature distribution in the boundary layer, when the Prandtl number (Pr) changes gradually. It shows that as the Prandtl number increases, the temperature of the boundary layer diminishes. This may be attributed to the fact that the thermal boundary layer thickness reduces with an increase in Prandtl number. Further, this figure indicates that the temperature gradient at the surface increases with a rise in Prandtl number. This implies that an increase in Prandtl number is accompanied by an enhancement of the heat transfer rate at the wall of the blood vessel. The underlying physics behind this can be described as follows. When blood attains a higher Prandtl number, its thermal conductivity is lowered down and so its heat conduction capacity diminishes. Thereby the thermal boundary layer thickness gets reduced. As a consequence, the heat transfer rate at the vessel wall is increased. Figure (12) illustrates the effect of the heat source parameter (Q) on the temperature. It is noticed that as the heat source parameter increases, the temperature decreases. Figure (13) illuminates a very important effect of thermal radiation on the temperature profile. This figure emphasizes that as thermal radiation increases during blood flow in capillaries; there is a significant rise in the thickness of boundary layer. Thereby the temperature of the boundary layer in enhanced by an appreciable extent.

The effects of order of chemical reaction on concentration distributions are displayed in figure (14) respectively. It is observed from these figures that an increase in the chemical reaction order n leads to decrease the concentration profiles. Figure (15) illustrate the effect of the Prandtl number on the concentration profiles respectively. It is evident that increases in the Prandtl number leads to increases on the concentration profiles.

From figure (16) Soret number (S_0) increases with increasing values on the concentration profiles. Figure (17) illustrate the concentration field distributions with transverse coordinate for different Schmidt number (Sc). An increase in Sc causes a considerable figure (17). A much greater reduction is observed in concentration values in figure (17). An increase in (Sc) will suppress concentration in the boundary layer regime.

Higher Sc will imply a decrease of molecular diffusivity D causing a reduction in concentration boundary layer thickness. Lower Sc will result in higher concentrations i.e. greater molecular (species) diffusivity causing an increase in concentration boundary layer thickness. For the highest value of Sc, the concentration boundary layer thicknesses are of the same value approximately i.e. both species and momentum will diffuse at the same rate in the boundary layer.

The effects of Soret number (S_0) versus Grashof number (Gr) on the local skin-friction coefficient shown in figure (18). From these figure we observe that the local skin-friction coefficient increase as Soret number (S_0)

CONCLUSIONS

The problem of steady laminar, hydromagnetic two-dimensional mixed convection flow due to stretching sheet in the presence of Soret effects was investigated. The resulting partial differential equations, describing the problem, are transformed into ordinary differential equations by using similarity transformations. These equations are more conveniently solved analytically by perturbation technique for the computation of flow, heat and mass transfer characteristics, skin-friction coefficient, for various values of the magnetic field parameter, heat source, Soret numbers, etc. Comparisons of the present results with previously published work on some limiting cases were performed and results were found to be in excellent agreement. From the present investigation following conclusions are drawn:

- Increasing the magnetic field parameter decreases the flow velocity near the stretching sheet in the momentum boundary layer, whereas its effect is reversed as the space variable of porous permeability parameter.
- Temperature deceases where as increases in radiation parameter.
- Skin friction increases with increase in the value of Soret number.
- Temperature decreases with increase in non-uniform heat source parameter
- Increase in the value of Schmidt number the concentration profiles decreases.

It is hoped that the present investigation is useful in the study of MHD flow over a vertical plate embedded in non-Darcian porous medium which can be utilized as the basis for many scientific and industrial applications and studying more complex problems involving Soret effects.

REFERENCES

[1] Ludwing (1856): The thermo diffusion phenomenon was discovered, *Akad. Wiss. Wien Math.-naturw.* Kl, 20: 539, pp. 551-555

[2] Soret (1879): and named as the Soret effect. The Soret coefficient is the ratio of the thermo diffusion coefficient to the molecular diffusion coefficient, *Arch. Geneve*, 3:48.

[3] Pal D and Talukdar B (2010). Buoyancy and chemical reaction effects on MHD mixed convection heat and mass transfer in a porous medium with thermal radiation and ohmic heating. *Communications in Nonlinear Science and Numerical Simulation,* 15(10), pp. 2878–2893.

[4] Mukhopadhyay S (2009): Effect of thermal radiation on unsteady mixed convection flow and heat transfer over a porous stretching surface in porous medium. *International Journal of Heat and Mass Transfer*, 52(13), pp. 3261–3265.

[5] Hayat T, Mustafa M and Pop I (2010): Heat and mass transfer for Soret and Dufour's effect on mixed convection boundary layer flow over a stretching vertical surface in a porous medium filled with a viscoelastic fluid. *Communications in Nonlinear Science and Numerical Simulation,* 15(5), pp. 1183–1196.

[6] M Bhavana, D Chenna Kesavaiah, A Sudhakaraiah (2013): The Soret effect on free convective unsteady MHD flow over a vertical plate with heat source, *International Journal of Innovative Research in Science, Engineering and Technology Vol. 2 (5),* pp. 1617-1628.

[7] D Chenna Kesavaiah, P V Satyanarayana, S Venkataramana (2013): Radiation and Thermo - Diffusion effects on mixed Convective heat and mass Transfer flow of a viscous dissipated fluid over a vertical surface in the presence of chemical reaction with heat source, *International Journal of Scientific Engineering and Technology.,* Vo.2(2), pp : 56-72.

[8] Rahman M M, Eltayeb I A and Rahman S M (2009): Thermo micropolar fluid flow along a vertical permeable plate with uniform surface heat flux in the presence of heat generation, *Thermal Science*, 13(1), pp. 23-36

[9] Ibrahim A A (2009): Analytic solution of heat and mass transfer over a permeable stretching plate affected by chemical reaction, internal heating, Dufour –Soret effect and hall effect, *Thermal Science*, 13 (2), pp. 183-97

[10] Pal D and Chatterjee S (2010): Heat and mass transfer in MHD non-Darcian flow of a micropolar fluid over a stretching sheet embedded in a porous media with non-uniform heat source and thermal radiation, *Commun., Nonlinear Sci., Numer., Simulat*., 15, pp. 1843-1857

[11] Cortell (2007): Viscous flow and heat transfer over a non-linear stretching sheet. *Applied Mathematics Compute,* Vol.184 (2), pp. 864 – 873.

[12] Raptis, A., and Perdikis, C. (2006): Viscous Flow over a non- linear stretching sheet in the Presence of a chemical reaction and magnetic field. *Int. J. Non-Linear Machinery*. Vol. 63, pp.527– 529.

[13] Rajagopal K R (1983): On Stokes problem for a non-Newtonian fluid. *Acta Mechanica*, Vol.48, pp.233-239.

[14] Shit G C and Haldar R (2009): Effect of thermal radiation on MHD viscoelastic fluid flow over a stretching sheet with variable viscosity. *Communicated for publication in Int. J. Fluid Mech.*

[15] Cogly A C, Vincentry W C and Gilles S E (1968): A Differential approximation for radiative transfer in a non-gray gas near equilibrium, *AIAA Journal*, 6

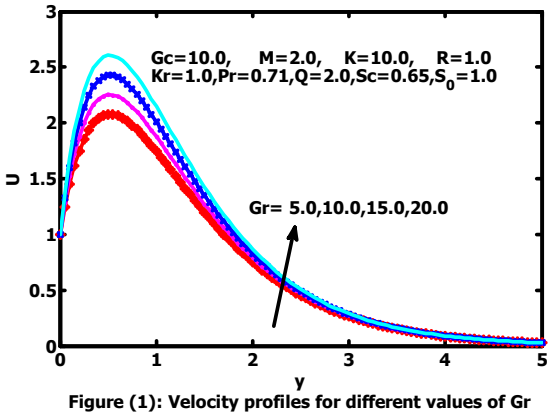

Figure (1): Velocity profiles for different values of Gr

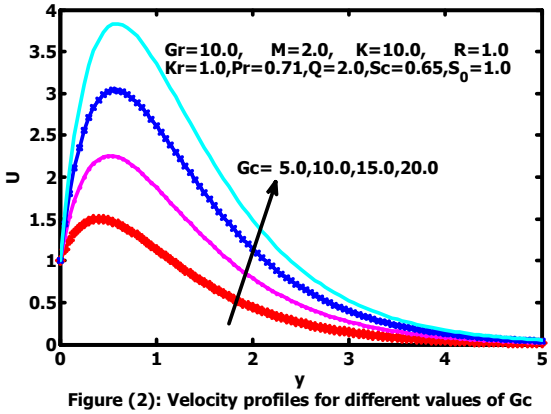

Figure (2): Velocity profiles for different values of Gc

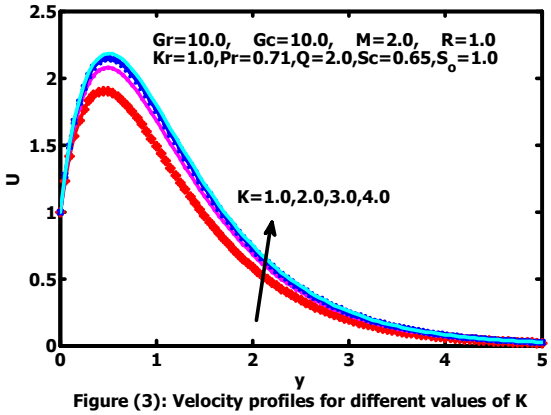

Figure (3): Velocity profiles for different values of K

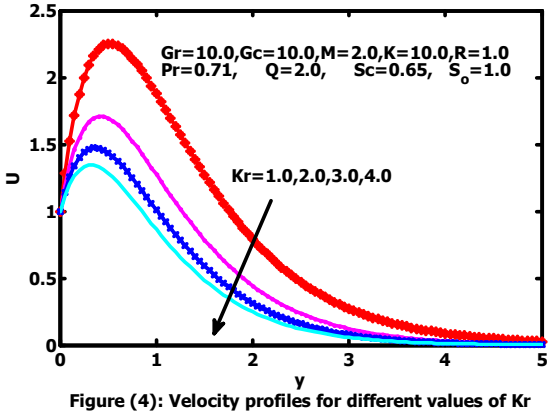

Figure (4): Velocity profiles for different values of Kr

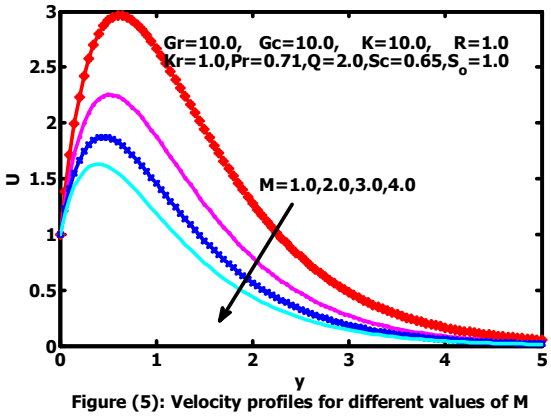

Figure (5): Velocity profiles for different values of M

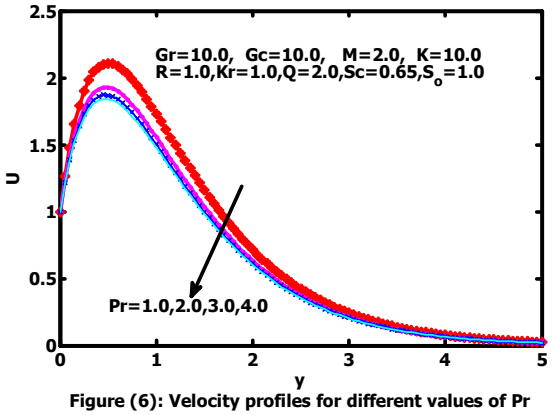

Figure (6): Velocity profiles for different values of Pr

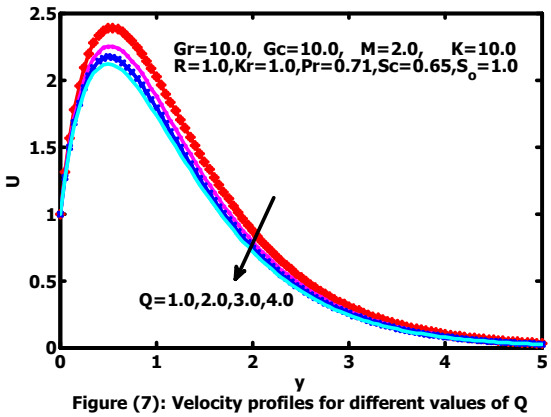

Figure (7): Velocity profiles for different values of Q

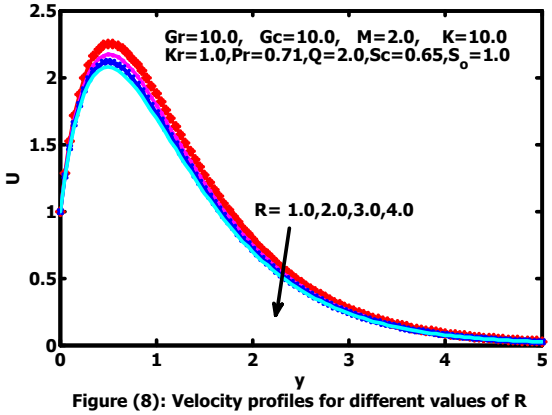

Figure (8): Velocity profiles for different values of R

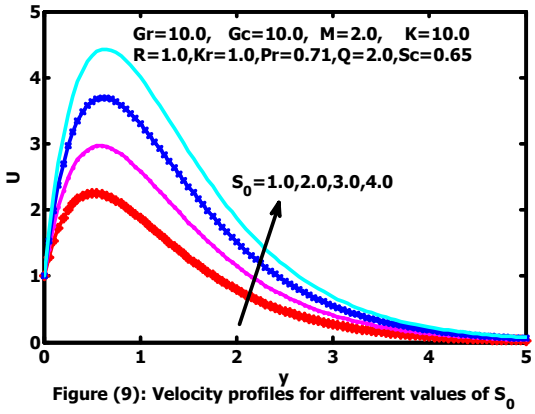

Figure (9): Velocity profiles for different values of S_0

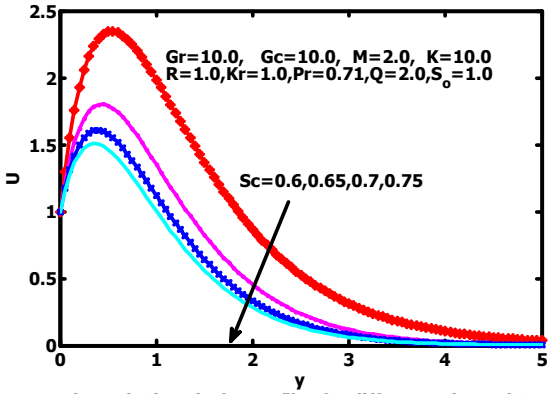

Figure (10): Velocity profiles for different values of Sc

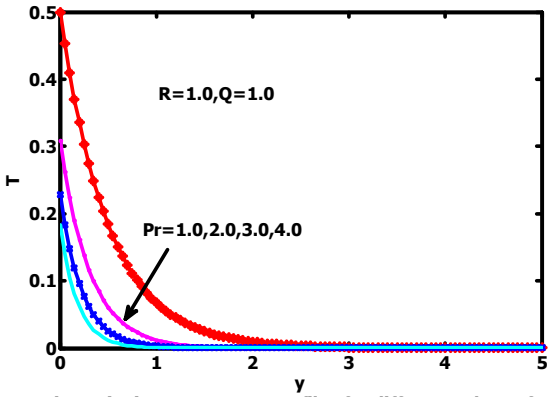

Figure (11): Temperature profiles for different values of Pr

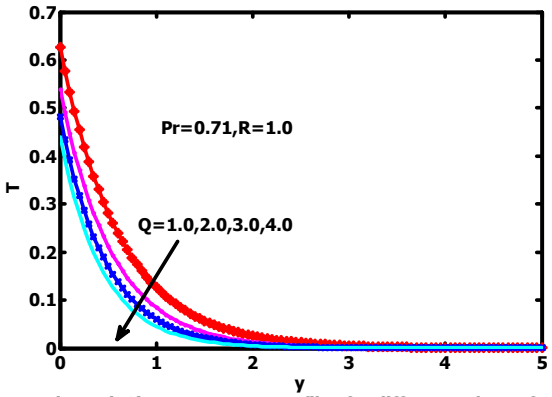

Figure (12): Temperature profiles for different values of Q

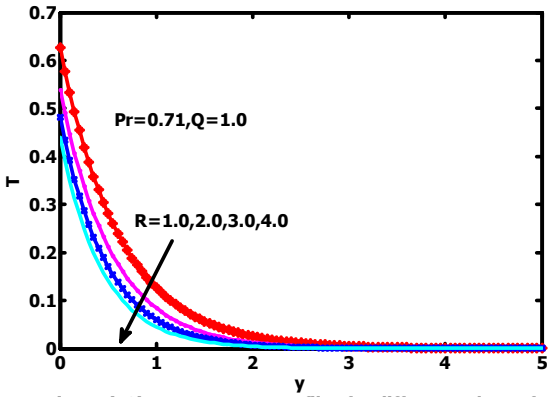

Figure (13): Temperature profiles for different values of R

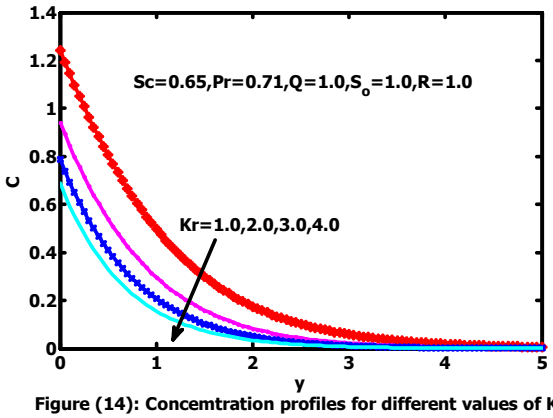

Figure (14): Concemtration profiles for different values of Kr

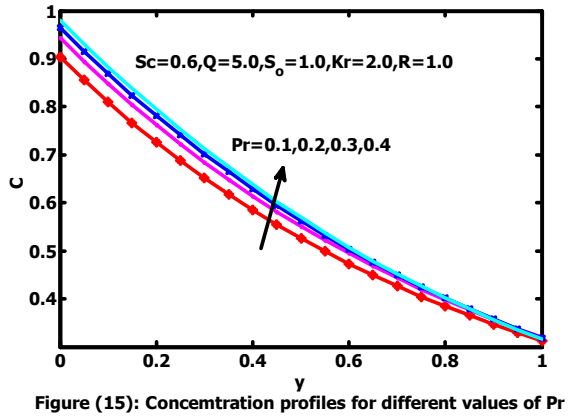

Figure (15): Concemtration profiles for different values of Pr

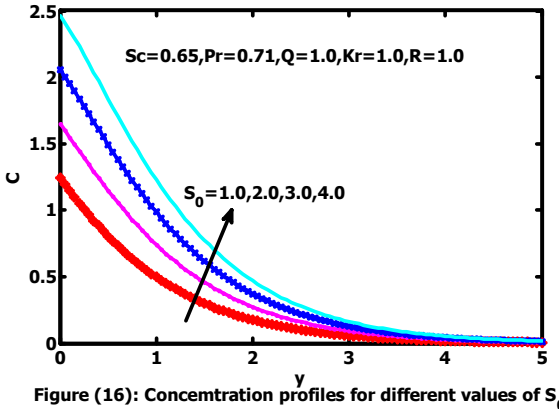

Figure (16): Concemtration profiles for different values of S_0

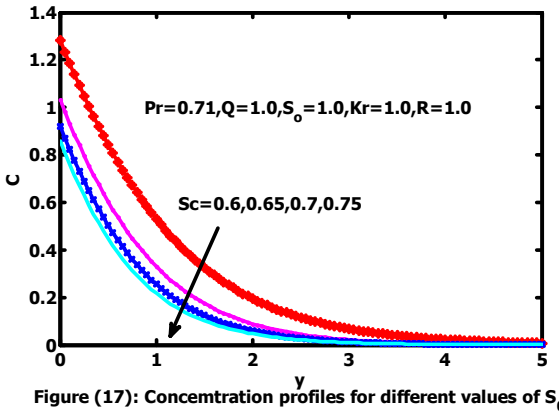

Figure (17): Concemtration profiles for different values of S_0

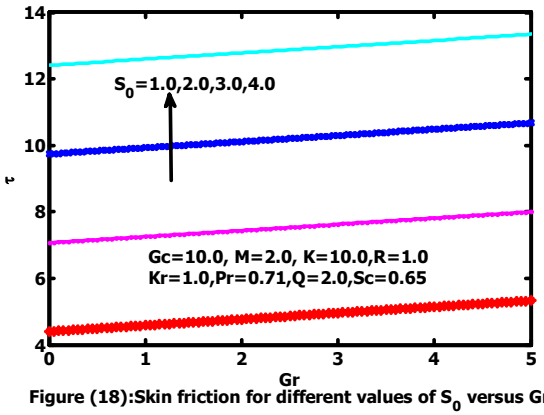

Figure (18):Skin friction for different values of S_0 versus Gr